Electronic Supplementary Material (ESI) for Journal of Materials Chemistry A.
This journal is © The Royal Society of Chemistry 2024

Supporting Information

π-π stacking small molecule enable high performance perovskite solar cells

Aoxi He, [a] Meng Wang, [a] Xiaoli Gong,[a] Peng Tang,[*b] Lili Wu,[a] Xia Hao, [a] Wenwu Wang, [a] Gengpei Xia,[c] Yu Jiang,[c] and Jingquan Zhang[*a]

[a]College of Materials Science and Engineering & Institute of New Energy and Low-carbon Technology, Sichuan University, Chengdu 610064, P.R. China

E-mail: zhangjq@scu.edu.cn

[b]Chengdu Textile College, Chengdu 611731, P.R. China

E-mail: TP.dayanyifeng@cdtc.end.cn

[c]National Photovoltaic Products Quality Supervision and Inspection Center, Chengdu Product Quality Supervision, Inspection and Research Institute, Chengdu 610100, P.R. China

Supporting information Part I

Experimental Section

Materials: SnO_2 colloid precursor (tin (IV) oxide, 15% in H_2O colloidal dispersion) was purchased from Alfa Aesar. Dimethylformamide (DMF), dimethyl sulfoxide (DMSO), chlorobenzene (CB), and acetonitrile were purchased from J&K Scientific Ltd. Caesium iodide (CsI), methylammonium iodide (MAI), and formamidinium iodide (FAI), Methylamine hydrochloride (MACl), lead iodide (99%) and lead bromide (99%), 4-tert-butylpyridine (tBP) and bis(trifluoromethane)sulfonimide lithium salt (Li-TFSI), phenethylammonium iodide (PEAI) and spiro-OMeTAD were purchased from Xi'an Polymer Light Technology Corp.; ITO glass was purchased from Suzhou Shang Yang Solar Technology Company.,Ltd. All the chemical materials were used as received unless stated otherwise.

Perovskite precursor preparation: CsI (22.1 mg/ml), FAI (263.1 mg/ml), MAI (13.5mg/ml), MACl (33mg/ml), PbI_2 (783.7 mg/ml) were dissolved in a DMF/DMSO = 4:1 solvent for the $FAMACsPbI_3$ precursor.

Device Fabrication: ITO substrates were sequentially rinsed by sonication in detergent, deionized (DI) water, acetone and ethanol, and finally dried in air. Then, cleaned ITO substrates were treated with ultraviolet–ozone for 15 min. The SnO_2 precursor was prepared by mixing SnO_2 (15% in a H_2O colloidal dispersion) and deionized water at a volume ratio of 1:3 for several hours and filtered by a 0.2 μm syringe filter before use. To form a SnO_2 layer, 100 μL of the SnO_2 precursor was

spin-coated (EZ6, made by JIANGSU LEBO SCIENCE) on the cleaned substrate at 4000 rpm for 30 s, which was heat-treated at 150 °C for 30 min. The SnO_2 coated substrates were further treated with UV–ozone before transferring into a glovebox for follow-up procedures. The perovskite precursor solution was spin coated on substrates following 2 steps: 1000 rpm for 5 s, 5000 rpm for 25 s. During the second step, 200 μL of chlorobenzene was drop-cast on substrates 5 s prior to the end of program. The substrates then were immediately annealed at 130 °C for 40 min. After that, PEAI (5 mg mL^{-1} in IPA) was spin-coated on the perovskite layer at 3000 rpm for 30s. After that, the spiro-OMeTAD solution was composed of 72.3 mg spiro-OMeTAD, 28.8 μL TBP, and 17.5 μL Li-TFSI solution (520 mg in 1 mL acetonitrile) in 1 mL chlorobenzene, and then spin-coated on perovskite film at 4000 rpm for 30 s. Finally, a 100 nm Au electrode was deposited by thermal evaporation.

Characterizations: The current density–voltage (J–V) curves were measured by a Keithley 2400 source meter unit under a solar simulator equipped with an AM 1.5G filter. Power density of the simulated solar light was calibrated to be 100 mW cm^{-2} with a standard silicon solar cell (certified by NREL). The active area of devices is 0.0576 cm^2 External quantum efficiency was measured by a solar cell spectral response measurement system (QER3-011, Enli Technology Co. Ltd., Taiwan). Morphologies of the perovskite films were observed by high-resolution field emission scanning electron microscopy (HR-FESEM) (FEI, Inspect F50). The crystalline structures for the perovskite films were characterized by X-ray diffraction (DX-2700,

Haoyuan Instrument Co., Ltd). Steady-state and time-resolved photoluminescence spectra were measured by a fluorescence spectrometer (FLS980, EI, England).

Supporting information Part II

1. Detailed theoretical simulation analysis models and calculation methods

The first-principles calculations were performed in the framework of DFT by the Cambridge Serial Total Energy Package (CASTEP) code[1]. The plane-wave ultrasoft pseudopotentials were employed to present the atoms [2] in perovskite calculation. Perdew-Burke-Ernzerhof (PBE) function within the generalized gradient approximation (GGA) was used to deal with the exchange and correlation terms during geometry optimization [3, 4] and the plane wave energy cutoff was set to be 2×2×2. For geometrical optimization, the total energy convergence was set less than 1×10^{-5} eV/atom.

1) The model used for calculation

When BAC molecules enter the crystal, there are three possibilities: only bromine atoms replace iodine in the lattice (model I), -COOH replaces iodine in the lattice (model II), and two functional groups simultaneously replace iodine in the lattice (model III). For PyI molecules, iodine on PyI can replace iodine in the perovskite lattice (Model IV). For 2-PL molecules, -COOH could replace iodine in the perovskite lattice (Model V). The specific model structure is shown in Figure S1. Figure S2 shows the calculation area of the effect of additives on the cell volume of perovskite at the center red box. We chose the area far from the doping center to calculate the cell volume change, which can better reflect the overall situation of the film.

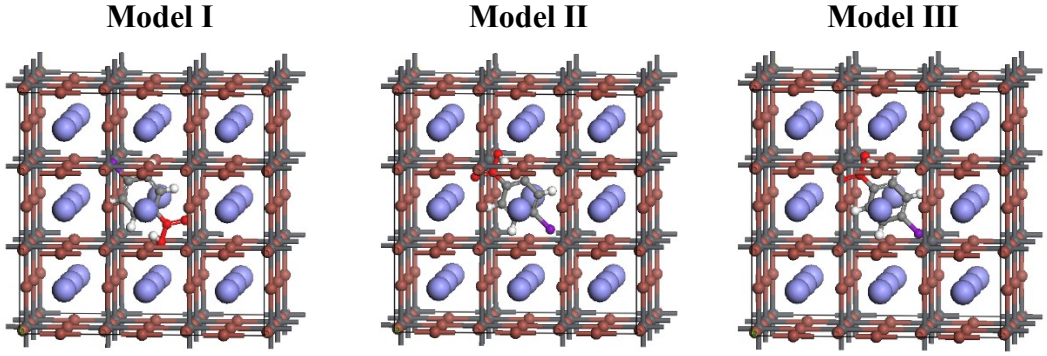

Model IV

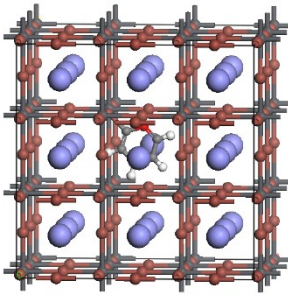

Model V

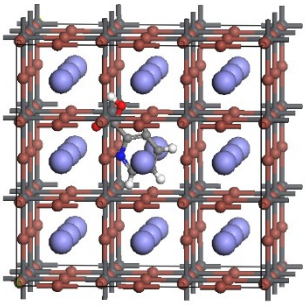

Figure S1 the model used for calculation

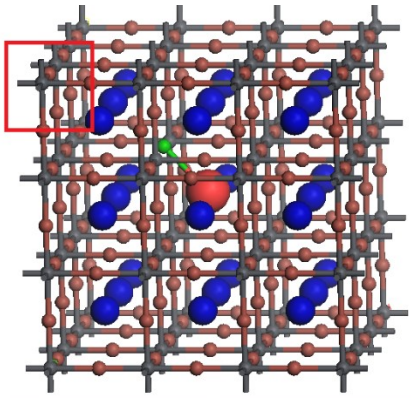

Figure S2 Calculation region of the effect of additives on the volume of perovskite crystal cells.

2. Result discussion

1) The effect of additives on the volume of perovskite crystal cells

Table S1 Volume of perovskite crystal cells with or without additives

Sample	**Crystal cells volume /$Å^3$**
Control	274.38
Model I	272.53
Model II	273.44
Model III	284.24
Model IV	279.42
Model V	281.96

2) The effect of BAC on α phase formation energy

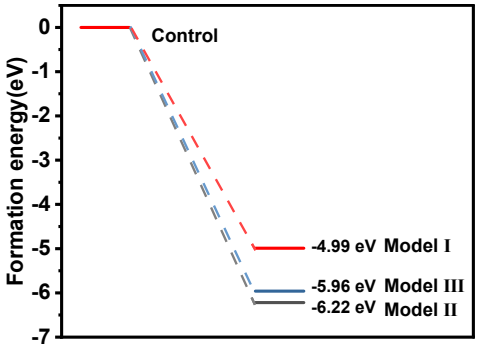

Figure S3 Calculation region of the effect of additives on the volume of perovskite crystal cells.

We calculated the α phase transformation energy of different models separately. The results indicate the α phase transformation energy of three different models decreased to -5.96 eV, -6.22 eV, and -4.99 eV respectively when the control serves as a reference point (i.e. 0 eV). Therefore, this result indicates that when BAC molecules enter the lattice, they are most likely to exist in the thin film in the form of -COOH replacing iodine in the lattice. And in this case, the crystal cell volume of the perovskite shrinks, which can effectively regulate the tensile strain of the perovskite film.

Supporting information Part III

Figures and Tables

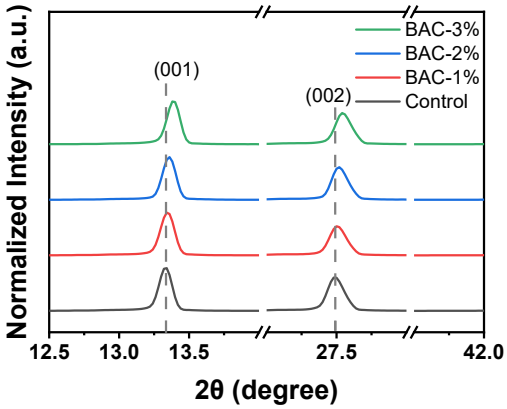

Figure S4 XRD patterns of films with different amounts of BAC additives

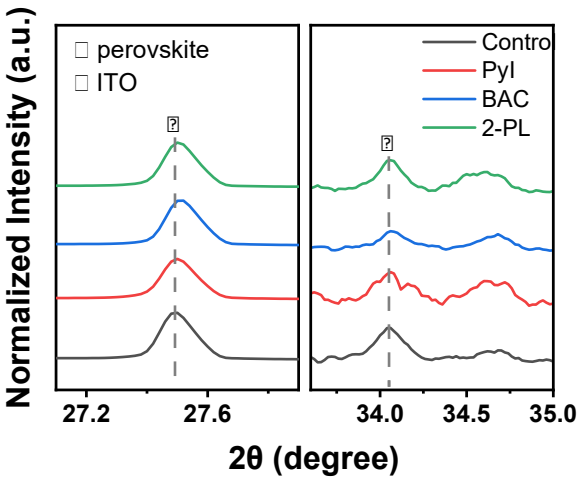

Figure S5 Close-up views of Figure 2e

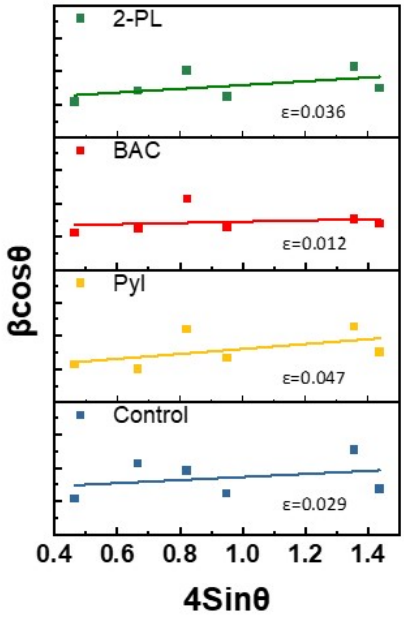

Figure S6 Williamson-Hall plots of films under different additive treatments.

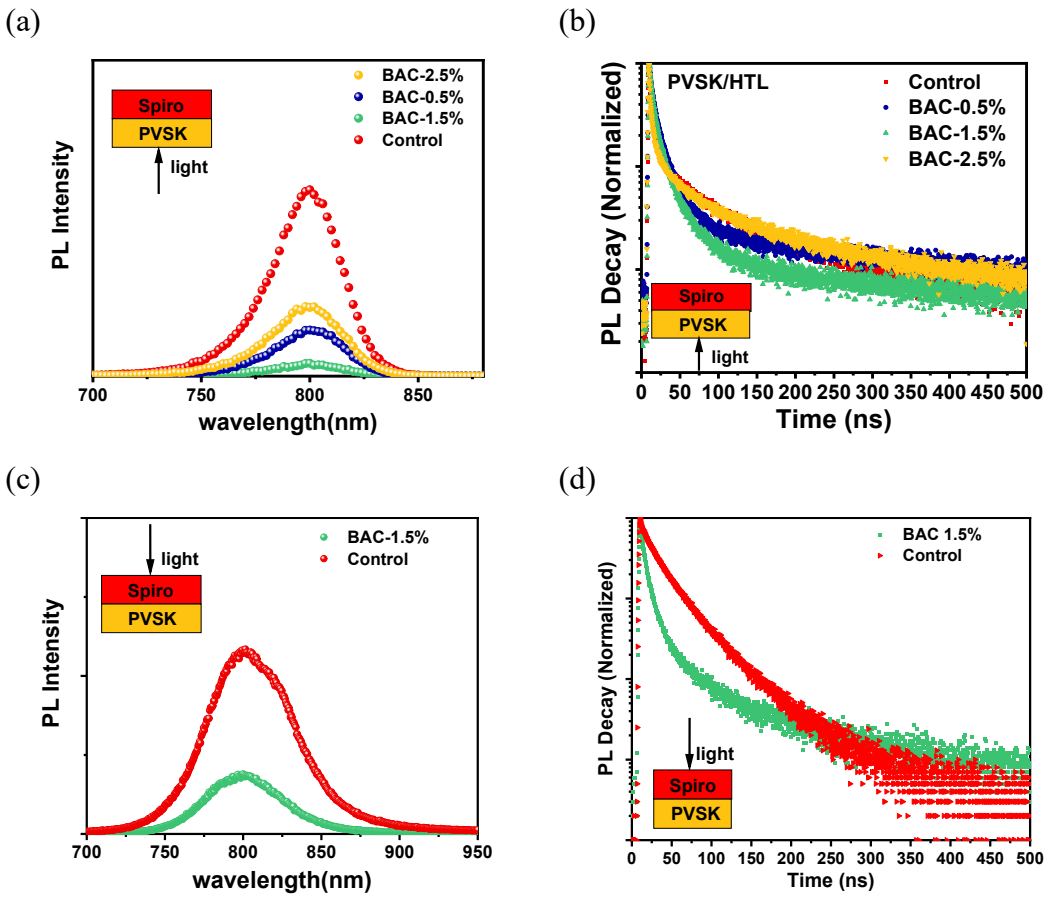

Figure S7 (a) and (b) PL spectra and TRPL decay curves of perovskite/HTL films (excitation is from PVSK side), (c) and (d) PL spectra and TRPL decay curves of perovskite/HTL films (excitation is from Spiro side)

Table S2 TRPL fitted parameters of perovskite films.

The PL decay was fitted using a biexponential decay function:

$$\tau_{ave} = Aexp\left(-\frac{t}{\tau_1}\right) + Bexp\left(-\frac{t}{\tau_2}\right) + C \quad (1)$$

Where A, B, and C are constants, t is PL decay time, τ_1 and τ_2 are fitted lifetimes. The average lifetime (τ_{ave}) was calculated using the following equation:

$$\tau_{ave} = \frac{A\tau_1^{\,2} + B\tau_2^{\,2}}{A\tau_1 + B\tau_2}$$

perovskite films

Sample	A	τ_1(ns)	B	τ_2(ns)	$\tau_{(avg)}$(ns)
Control	10.96	32.82	89.04	346.49	342.87
0.5% BAC	1.65	10.00	98.35	522.42	522.26
1.5% BAC	4.97	31.89	95.03	576.61	575.04
2.5% BAC	12.98	28.02	87.02	224.87	221.28

HTL/PVSK (excitation is from PVSK side)

Sample	A	τ_1(ns)	B	τ_2(ns)	$\tau_{(avg)}$(ns)
Control	23.99	3.06	76.01	61.81	52.11
0.5% BAC	44.54	6.08	55.06	30.56	16.20
1.5% BAC	42.46	5.15	57.54	25.44	14.55
2.5% BAC	19.32	3.10	80.68	60.95	55.91

HTL/PVSK (excitation is from Spiro side)

Sample	A	τ_1(ns)	B	τ_2(ns)	$\tau_{(avg)}$(ns)
Control	64.15	14.16	35.85	48.14	36.42
1.5% BAC	63.07	10.2	36.93	14.67	12.24

For the PL and TRPL spectra of HTL/PVSK sample, we conduct the excitation from Perovskite and Spiro side respectively. The results indicate that the trend of PL and TRPL spectra characteristics are basically consistent under the testing conditions of the two incident directions.

Similar to crystalline silicon materials, the signals intensity of PL and TRPL is determined by the bulk phase, the surface near the substrate, and the surface exposed to air[5]. Similar with QSSPC method to characterize the minority carrier lifetime of

crystalline silicon, the possible differences in test results caused by the direction of excitation light depend on the absorption depth of the material under the excitation light used, the diffusion length of photo generated non-equilibrium carriers, and the carrier recombination characteristics of the surface in the incident direction and the opposite direction[5, 6]. In this paper, due to the excitation light wavelength used in the test being 650nm, the absorption coefficient corresponding to 650nm can be obtained from the transmittance spectrum shown in Figure S6 and thickness (750nm) of the thin film, which is 41000-42000. Therefore, the corresponding absorption depth can be obtained to be about 230nm. The absorption depth corresponding to the excitation light used reaches one-third of the sample thickness. Therefore, whether the excitation is from PVSK side or the Spiro side, the lifetime of photo-generated non-equilibrium carriers is determined by the surface and the thin film inside. Due to the glass isolating the contact between perovskite and the environment, the carrier recombination rate at glass/PVSK interface is low. Furthermore, due to the selective hole transport effect of the Spiro/perovskite interface, which suppresses the carrier recombination rate at this interface, the excitation light mainly reflects the bulk recombination of the perovskite film when incident from the glass surface and Spiro surface, respectively. Therefore, the trend of PL and TRPL spectra characteristics are basically consistent under the testing conditions of the two incident directions.

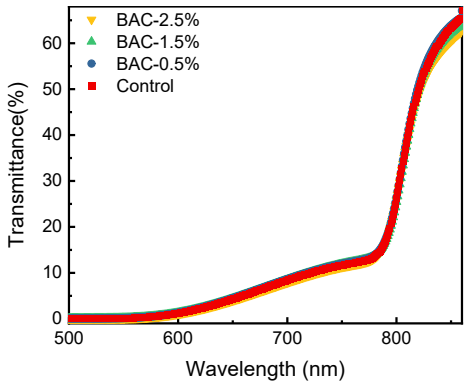

Figure S8 UV-vis absorption spectra of control group and BAC-modified perovskite films

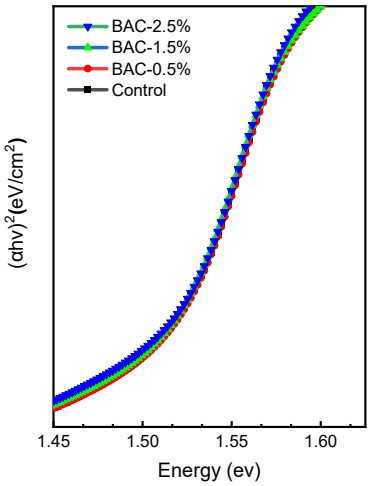

Figure S9 Comparison of Tauc plots for the control group and BAC-modified perovskite films

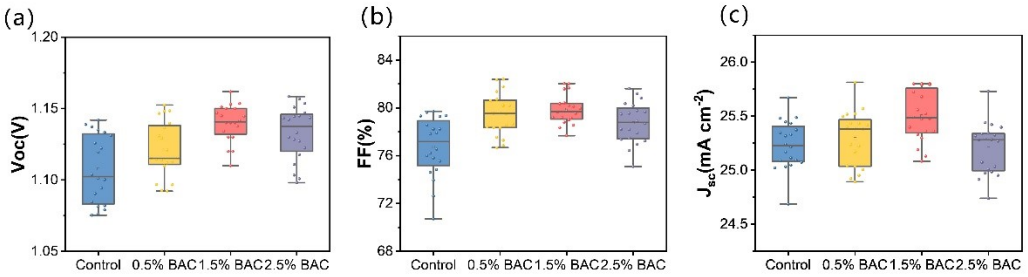

Figure S10 Photovoltaic parameters statistical chart of control group and BAC-modified perovskite solar cells: (a) Voc, (b) FF, (c) Jsc.

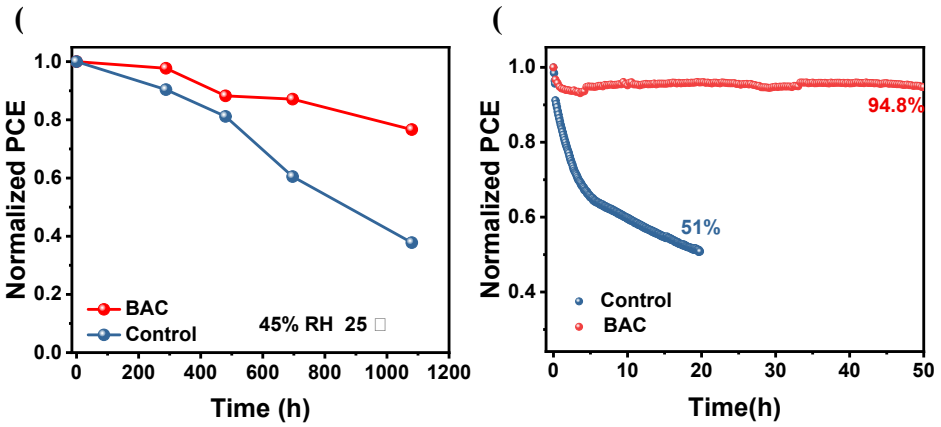

Figure S11. (a) Normalized PCE variation curves of the unencapsulated control and BAC perovskite devices. (b) Maximum power point tracking.

1. M. D. Segall, P. J. D. Lindan, M. J. Probert, C. J. Pickard, P. J. Hasnip, S. J. Clark and M. C. Payne, *Journal of Physics: Condensed Matter*, 2002, **14**, 2717-2744.
2. K. Laasonen, A. Pasquarello, R. Car, C. Lee and D. Vanderbilt, *Phys Rev B Condens Matter*, 1993, **47**, 10142-10153.
3. J. P. Perdew, K. Burke and M. Ernzerhof, *Phys Rev Lett*, 1996, **77**, 3865-3868.
4. Y. Zhang and W. Yang, *Physical Review Letters*, 1998, **80**, 890-890.
5. Kalogirou, Soteris, ed. McEvoy's handbook of photovoltaics: fundamentals and applications. Academic Press, 2017
6. I. Martin, A. Alcaniz, A. Jimenez, G. Lopez, C. del Canizo and A. Datas, *IEEE Journal of Photovoltaics*, 2020, **10**, 1068-1075.